Stem Cell Reports
Article

OPEN ACCESS

Epigenetic Modification of the CCL5/CCR1/ERK Axis Enhances Glioma Targeting in Dedifferentiation-Reprogrammed BMSCs

Rui Chen,[1,2] Wayne Yuk-Wai Lee,[3] Xiao Hu Zhang,[1,2] Jie Ting Zhang,[1,2] Sien Lin,[3] Liang Liang Xu,[3] Biao Huang,[1,2] Fu Yuan Yang,[1,2] Hai Long Liu,[1,2] Bin Wang,[3] Lai Ling Tsang,[1,2] Sandrine Willaime-Morawek,[5] Gang Li,[3,4] Hsiao Chang Chan,[1,2,4,*] and Xiaohua Jiang[1,2,4,*]

[1]Key Laboratory for Regenerative Medicine, Ministry of Education, School of Biomedical Sciences
[2]Epithelial Cell Biology Research Center
[3]Department of Orthopaedics & Traumatology
Faculty of Medicine, The Chinese University of Hong Kong, Hong Kong SAR, PR China
[4]The Chinese University of Hong Kong, Shenzhen Research Institute, Shenzhen 518057 PR China
[5]Clinical Neurosciences, Faculty of Medicine, University of Southampton, Southampton SO16 6YD, UK
*Correspondence: hsiaocchan@cuhk.edu.hk (H.C.C.), xjiang@cuhk.edu.hk (X.J.)
http://dx.doi.org/10.1016/j.stemcr.2017.01.016

SUMMARY

The success of stem cell-mediated gene therapy in cancer treatment largely depends on the specific homing ability of stem cells. We have previously demonstrated that after in vitro induction of neuronal differentiation and dedifferentiation, bone marrow stromal cells (BMSCs) revert to a primitive stem cell population (De-neu-BMSCs) distinct from naive BMSCs. We report here that De-neu-BMSCs express significantly higher levels of chemokines, and display enhanced homing abilities to glioma, the effect of which is mediated by the activated CCL5/CCR1/ERK axis. Intriguingly, we find that the activated chemokine axis in De-neu-BMSCs is epigenetically regulated by histone modifications. On the therapeutic front, we show that De-neu-BMSCs elicit stronger homing and glioma-killing effects together with cytosine deaminase/5-fluorocytosine compared with unmanipulated BMSCs in vivo. Altogether, the current study provides an insight into chemokine regulation in BMSCs, which may have more profound effects on BMSC function and their application in regenerative medicine and cancer targeting.

INTRODUCTION

Mesenchymal stem cells (MSCs) are self-renewing, multipotent progenitor cells with the potential to differentiate into different cell types such as osteoblasts, chondrocytes, neurons, cardiomyocytes, hepatocytes, and epithelial cells (Uccelli et al., 2008). Due to their accessibility, multipotency, and convenient expansion protocols, MSCs have been recognized as promising candidates for cellular therapy in regenerative medicine and tissue repair (Caplan, 2007; Uccelli et al., 2008). In fact, MSC transplantation is considered safe and has been widely applied in clinical trials of cardiovascular (Ripa et al., 2007), neurological (Lee et al., 2008), and immunological diseases (Kim et al., 2013; Lazarus et al., 2005) with encouraging results. On the other hand, due to their inherent tumor-homing behavior, MSCs are considered advantageous for delivering anti-tumor agents as an adjuvant therapy for different types of cancer (Hong et al., 2009; Kim et al., 2008; Kosaka et al., 2012; Nakamizo et al., 2005; Nakamura et al., 2004; Ryu et al., 2012). Accumulating evidence has shown that MSCs can deliver various therapeutic agents, such as interleukin-2 (IL-2) (Nakamura et al., 2004), IL-12 (Hong et al., 2009), tumor necrosis factor (TNF)-related and apoptosis-inducing ligand (Kim et al., 2008), and suicide genes (Kosaka et al., 2012; Ryu et al., 2012) selectively to tumor loci, and that such delivery elicits a significant anti-tumor effect in animal models. However, it should be noted that the success of such treatment strategies largely depends on the migratory and homing ability of MSCs. Thus, a complete understanding of the molecular mechanisms underlying migration of MSCs toward target tissues is essential for improving the therapeutic application of MSCs.

Homing of transplanted MSCs into injured tissue or tumors is regulated by multiple processes that include cell attachment and rolling in the vessel lumen, adhesion and extravasation across the vascular endothelium, and migration through the tissue stroma (Eseonu and De Bari, 2015). Although the molecular mechanisms that govern directed migration of MSCs are not fully understood, there is an accumulating body of evidence showing that chemotactants, such as chemokines, cytokines, and growth factors, play a crucial role in the homing ability of circulating MSCs to injured tissues or tumors (Eggenhofer et al., 2014; Marquez-Curtis et al., 2014; Vanden Berg-Foels, 2014). Interaction between chemotactants and their receptors leads to multiple intracellular events that allow extravasation of cells from circulation and directional migration toward the area with the highest chemotactic gradient (Alexeev et al., 2013). Chemokine (C-C motif) ligand 5 (CCL5, also known as RANTES [regulated upon activation, normal T cell-expressed and secreted]), is secreted by various cell types including platelets, immune cells, fibroblasts, and endothelial and epithelial cells (Lin et al., 2013), and has been

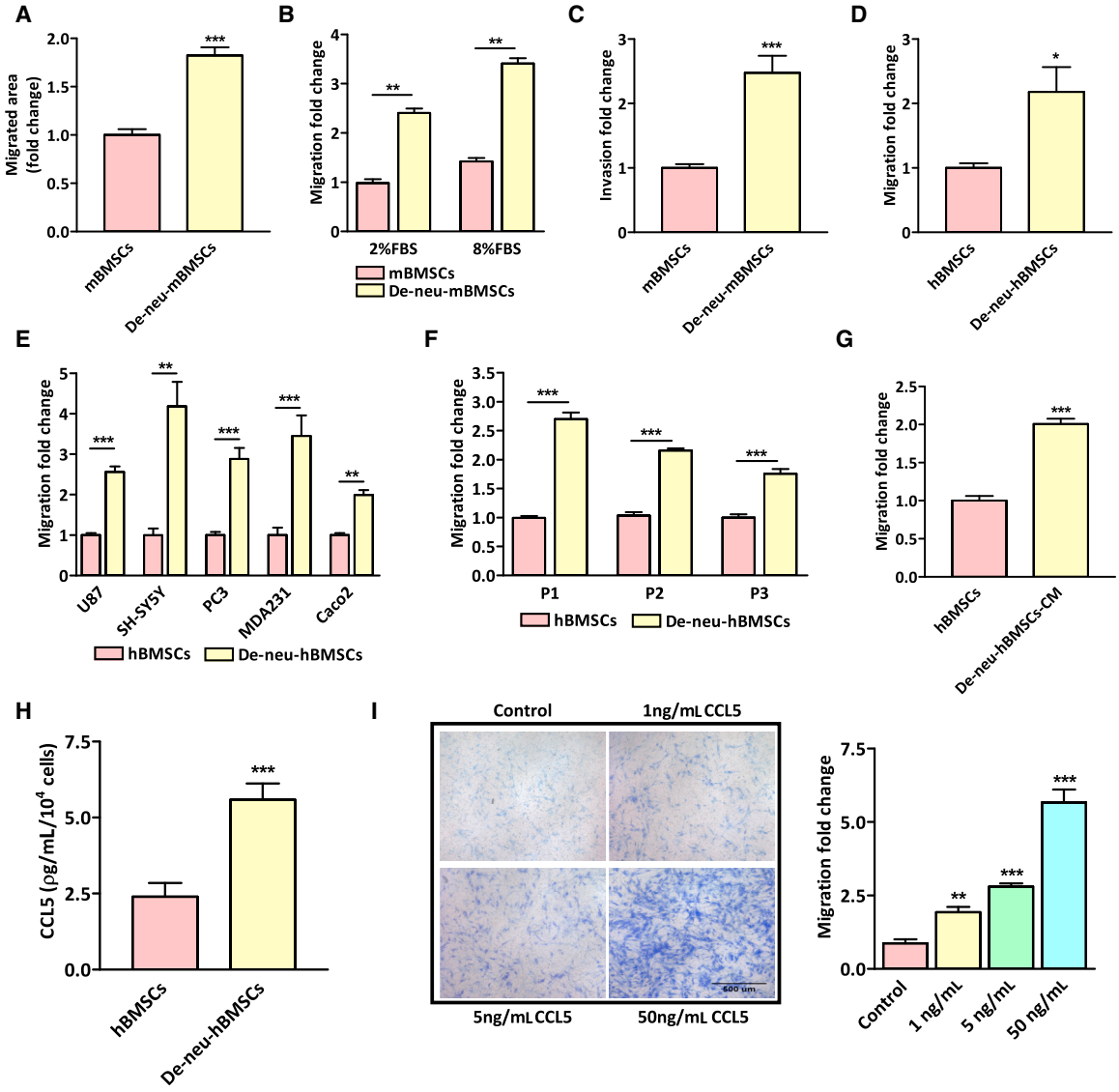

Figure 1. Enhanced Migratory and Homing Abilities in Human and Mouse De-neu-BMSCs

(A) Cell scratch assay in mBMSCs and De-neu-mBMSCs showing enhanced cell migration in De-neu-mMSCs. Quantification data are presented as means ± SD from three independent experiments (***$p < 0.001$).

(B) Transwell analyses showing that De-neu-mBMSCs migrated more to different concentrations of FBS compared with mBMSCs. Quantification data are presented as means ± SD from three independent experiments (**$p < 0.01$).

(C) De-neu-mBMSCs exhibited enhanced cell invasion compared with mBMSCs. Quantification data are presented as means ± SD from three independent experiments (***$p < 0.001$).

(D) A total of 2.5×10^4 hBMSCs/De-neu-hBMSCs were seeded in 200 μL of serum-free medium in the upper chamber and evaluated their migratory ability to 10% FBS medium using transwell assay. Quantification data are shown as fold change relative to hMSCs and presented as means ± SD from three independent experiments (*$p < 0.05$).

(E) A total of 2.5×10^4 hBMSCs/De-neu-hBMSCs were seeded in 200 μL of serum-free medium in the upper chamber and their migratory ability to the conditional medium collected from 1.8×10^6 cancer cells evaluated. Quantification data are shown as fold changes relative to hBMSCs and presented as means ± SD from three independent experiments (**$p < 0.01$, ***$p < 0.001$, t test compared with hBMSCs).

(F) hBMSCs and De-neu-hBMSCs were passaged in vitro for three passages and their migratory ability toward U87 CM by transwell assay evaluated. Quantification data are shown as fold change relative to hBMSCs and presented as means ± SD from three independent experiments (***$p < 0.001$).

(legend continued on next page)

originally identified as an inducer that can recruit leukocytes to sites of inflammation (Donlon et al., 1990). After binding to its receptors, namely CCR1, CCR3, and CCR5, CCL5 induces phosphorylation of mitogen-activated protein kinase and other signaling pathways involved in the regulation of various cellular functions, such as proliferation, migration, and differentiation (Aldinucci and Colombatti, 2014; Marques et al., 2013). Interestingly, it has been reported that the CCL5/CCR1 axis is critical for maintaining MSC identity and multipotency (Kauts et al., 2013). In addition, more recent studies have demonstrated that the CCL5/CCR1 signal is pivotal for the recruitment of MSCs toward inflammatory tissues and subsequent therapeutic effects (Lu et al., 2015; Wise et al., 2014). These findings raise fundamental questions as to how the CCL5/CCR1 axis is regulated, and how this axis controls MSC access to the target sites.

Dedifferentiation has been considered as one of the mechanisms rerouting cell fate by reverting differentiated cells to an earlier, more primitive phenotype. Interestingly, previous studies from both our group and others have demonstrated that dedifferentiation is a prerequisite for bone marrow stromal cells (BMSCs) to change their cell fate and re-differentiate into a different linage (Liu et al., 2010; Poloni et al., 2012). In addition, our recent studies demonstrated that MSCs derived from rat bone marrow (rBMSCs) could be reprogrammed in vitro via differentiation and dedifferentiation with enhanced therapeutic efficacy in tissue repair (Liu et al., 2011; Rui et al., 2015). Interestingly, our microarray profiling and gene ontology analysis reveals that the genes involved in cell motility and migration are differentially expressed between De-neu-rBMSCs and unmanipulated rBMSCs (Liu et al., 2011). Thus, we undertook the present study to evaluate the effect of dedifferentiation-mediated reprogramming on the migratory capability of BMSCs and their efficacy in glioma targeting and killing.

RESULTS

Enhanced Migratory and Homing Abilities in De-neu-BMSCs

In this study, we expanded our study to both human and mouse BMSCs and demonstrated that De-neu-h/mBMSCs exhibited enhanced cell survival and neuronal potentiality (Figures S1A–S1E), as observed previously in De-neu-rBMSCs (27). We then proceeded to evaluate the effect of dedifferentiation on the migratory ability of BMSCs. Our results showed that both dedifferentiated human and mouse BMSCs exhibited enhanced migratory and invasive ability as demonstrated by wound healing, transwell, and invasion assays (Figures 1A–1D). Next, various genes involved in cell migration, invasion, and motility were compared between hBMSCs and De-neu-hBMSCs using focused PCR array (Sabiosciences, PAHS 090Z). The result showed that the expression of matrix remodeling proteins, such as *mmp3* and *mmp9*, was significantly increased, whereas the expression of adhesion molecules, such as *cdh1*, *cola2*, *col3a1*, *col5a2*, *ocln*, and *krt14*, was decreased in De-neu-hBMSCs (Figure S1G), documenting a more mobile and invasive phenotype of De-neu-hBMSCs. Since the dedifferentiated BMSCs presented enhanced migratory and invasive ability, we speculated that De-neu-h/mBMSCs might exhibit a stronger homing capacity toward cancer cells. To test this possibility, we first examined the migratory ability of dedifferentiated hBMSCs and naive hBMSCs toward the conditional medium originated from different human cancer cell lines using transwell migration assays. Our results showed that De-neu-hBMSCs elicited a more robust homing response toward various cancer cell lines than that of hBMSCs, which can be maintained with prolonged passaging (Figures 1E and 1F). This enhanced tumor tropism is present in dedifferentiated mouse BMSCs as well (Figure S1F). Collectively, these results indicate that De-neu-BMSCs of human or mouse origin display enhanced migratory and tumor-homing abilities.

Autocrine CCL5 Signaling Promotes Migration in De-neu-BMSCs

Since MSC-mediated gene delivery has been shown to be a promising strategy for improving the efficacy and minimizing the toxicity of gene therapy in glioma treatment (Egea et al., 2011; Hong et al., 2009; Kim et al., 2008; Nakamizo et al., 2005; Nakamura et al., 2004), we decided to focus on the enhanced migratory ability in dedifferentiated BMSCs toward glioma in the following studies. Of note, we

(G) hBMSCs were treated with De-neu-hBMSCs CM for 48 hr, and their migration ability toward U87 CM was determined by transwell assay. Quantification data are shown as fold change relative to hBMSCs and presented as means ± SD from three independent experiments (***$p < 0.001$).

(H) CCL5 secretion in hBMSCs and De-neu-hBMSCs was examined by ELISA. Quantification data are presented as means ± SD from three independent experiments (***$p < 0.001$).

(I) hBMSCs were treated with different concentrations of recombinant human CCL5 for 24 hr in the upper chamber, and their migratory ability toward U87 CM, which was added to the lower chamber in the transwell assay, was determined. The result showed that exogenous administration of CCL5 enhanced hBMSCs migration toward U87 CM in a dose-dependent manner. Left: images showing the effect of CCL5 on BMSC migration. Right: quantification data are presented as means ± SD from three independent experiments (**$p < 0.01$, ***$p < 0.001$). Scale bar, 500 μm.

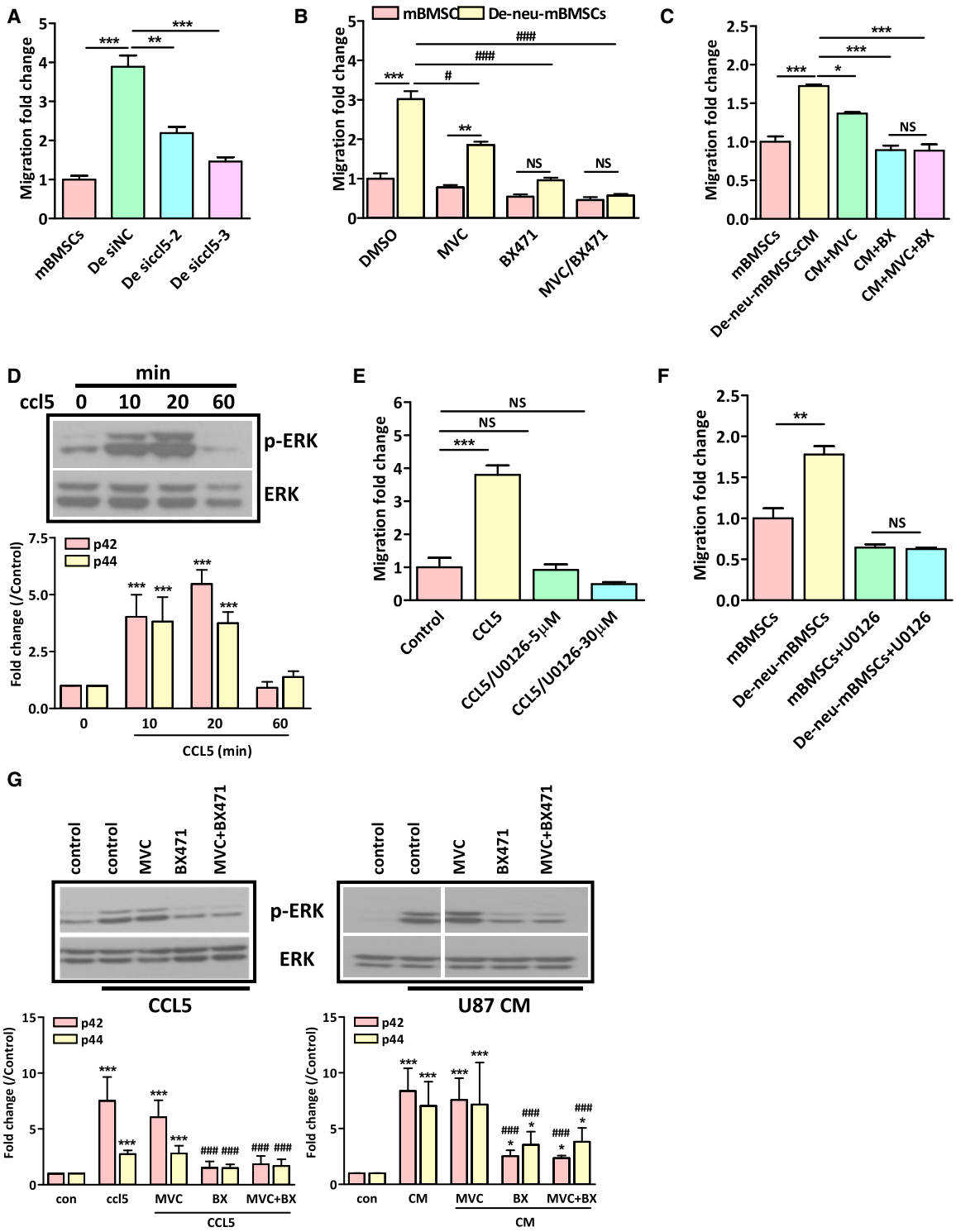

Figure 2. The Enhanced Migratory Capacity in De-neu-BMSCs Is Mediated by the Autocrine CCL5/CCR1/ERK Pathway

(A) mBMSCs were induced to undergo differentiation and dedifferentiation, and transfected with control or *ccl5* siRNAs (100 nM). After 24 hr of scrambled or *ccl5* siRNA treatment, mBMSCs or De-neu-mMSCs were plated in the upper chamber and their migratory ability toward U87 CM evaluated by transwell assay. Quantification data are presented as means ± SD from three independent experiments (**p < 0.01, ***p < 0.001).

(legend continued on next page)

found that incubation with the CM originated from De-neu-hBMSCs significantly increased migratory ability of hBMSCs toward U87 to a level similar to De-neu-hBMSCs (Figure 1G), indicating that secretion-borne factors in De-neu-hBMSCs may play an important role in the enhancement of their migratory capability. We therefore compared the expression levels of various chemokines and cytokines between BMSCs and De-neu-BMSCs using pathway-focused PCR array, and found that the expression of multiple chemokines and chemokine receptors including *ccl11*, *ccl12*, *ccl2*, *ccl4*, *ccl5*, *cxcl1*, *cxcl10*, *cxcl11*, *ccr3*, and *ccr8* was higher in De-neu-BMSCs compared with BMSCs (Figures S2A and S2B). Most notably, *ccl5* was expressed at a very high level in De-neu-hBMSCs compared with naive hBMSCs. The dramatic increase of *ccl5* mRNA expression led to a significant increase of CCL5 secretion in De-neu-hBMSCs (Figure 1H). To illustrate a direct effect of CCL5 on hBMSC migration toward glioma, we treated BMSCs with different concentrations of recombinant CCL5 in the upper chamber, and determined their migratory ability toward U87 CM, which was added to the lower chamber in the transwell assay. The result showed that exogenous administration of CCL5 enhanced hBMSCs migration toward U87 CM in a dose-dependent manner (Figure 1I). Due to the limited source of human BMSCs and the demand for large amounts of cells for biochemical study, we decided to use mouse BMSCs in the following mechanistic study. To further validate the causative role of autocrine CCL5 signaling in De-neu-mBMSCs migration, we took a loss-of-function approach by using *ccl5* small interfering RNAs (siRNAs). For *ccl5* knockdown experiments, De-neu-mBMSCs were transfected with *ccl5* siRNAs or control siRNA, and placed in the upper chamber. We were able to reduce the level of *ccl5* expression by more than 50-fold using two different siRNAs without any adverse effects on cell viability (Figure S2C). Our result showed that the increased migratory ability toward U87 CM in De-neu-mBMSCs was significantly decreased by *ccl5* siRNA treatment (Figure 2A). Taken together, these data indicate that the migratory capacity of De-neu-BMSCs was predominantly mediated by CCL5 signaling in an autocrine fashion.

The Effect of CCL5 on Migration Is Mediated by CCR1 and ERK in De-neu-BMSCs

CCL5 has three receptors, namely, CCR1, CCR3, and CCR5, whereas it mainly binds to CCR1 and CCR5 in MSCs (Gibon et al., 2012; Kauts et al., 2013; Li et al., 2012). To further determine through which receptor CCL5 exerted its effect on MSC migration, we took advantage of CCR1- and CCR5-specific inhibitors. To do this, mBMSCs or De-neu-mBMSCs were pre-treated with CCR1 inhibitor BX471 and/or CCR5 inhibitor MVC and added in the upper chamber, whereas U87 CM was administered in the lower chamber. Our results showed that, while MVC mildly affected the migratory capability of mBMSCs/De-neu-mBMSCs, BX471 attenuated the enhanced migratory capability in De-neu-mBMSCs, indicating that the enhanced chemotactic activity was largely CCR1 dependent (Figure 2B). Consistently, the De-neu-mBMSCs CM-induced cell migration could be completely reversed by BX471, but only mildly by MVC. Of note, the combination of both inhibitors did not have a synergistic effect, implying the minimal involvement of CCR5 (Figure 2C). Since it has been shown that the interaction between CCL5 and CCR1 can activate the ERK pathway, which is critical for cell migration (Kauts et al., 2013; Tian et al., 2004, 2008), we proceeded to examine the effect of CCL5 on ERK activation in mBMSCs. The result showed that treatment with recombinant CCL5 rapidly phosphorylated ERK1/2 at 10 min, but decreased after 1 hr (Figure 2D). Of note, suppression of ERK activity by an ERK inhibitor (5 μM, U0126) completely abrogated the

(B) The migratory ability toward U87 CM in mBMSCs/De-neu-mBMSCs after treatment with MVC and BX471 (1 μM pre-treatment for 24 hr followed by 2 μM treatment during transwell assay) was determined by transwell assay. Quantification data are presented as means ± SD from three independent experiments (**$p < 0.01$, ***$p < 0.001$ versus mMSCs; $^{\#}p < 0.05$, $^{\#\#\#}p < 0.001$ versus De-neu-mMSCs + DMSO). NS, not significant.

(C) CCR antagonists (1 μM pre-treatment for 24 hr followed by 2 μM treatment during transwell assay) were added simultaneously with CM of De-neu-mBMSCs into mBMSCs. The migratory ability toward U87 was determined by transwell assay. Quantification data are presented as means ± SD from three independent experiments (*$p < 0.05$, ***$p < 0.001$).

(D) mBMSCs were treated with 50 ng/mL CCL5 and the expression of total and phosphorylated ERK was determined by western blot. Quantification of p42/44 MAPK is shown in the lower panel, ***$p < 0.001$.

(E) The mBMSCs were treated with different concentration of U0126 and 50 ng/mL CCL5 for 24 hr, and then their migratory ability toward U87 CM was determined. Quantification data are presented as means ± SD from three independent experiments (***$p < 0.001$).

(F) Both mBMSCs and De-neu-mBMSCs were treated with U0126 (10 μM) and examined for their migratory ability toward U87 CM. Quantification data are presented as means ± SD from three independent experiments (**$p < 0.01$).

(G) Western blot analysis of ERK phosphorylation in BMSCs pre-treated with CCL5 receptor antagonist MVC and/or BX741 (1 μM), and followed by CCL5 (50 ng/mL) or U87 CM. Quantification of p42/44 MAPK is shown in the lower panel (*$p < 0.05$, ***$p < 0.001$ compared with control, $^{\#\#\#}p < 0.001$ compared with CCL5 treatment only).

CCL5-stimulated migration in mBMSCs (Figure 2E). To further elucidate the causative role of the ERK signaling pathway in the enhanced migration exhibited by De-neu-mBMSCs, we treated either mBMSCs or De-neu-mBMSCs with U0126, and examined their migratory capability toward U87 CM. Our results showed that 5 μM U0126 completely attenuated the enhanced migratory migration in De-neu-mBMSCs (Figure 2F), indicating that the augmented homing ability observed in De-neu-mBMSCs is attributable to the activation of the ERK pathway. Moreover, ERK phosphorylation was determined in mBMSCs treated with CCL5 along with its receptor antagonists. As shown in Figure 2G, CCL5- or U87 CM-induced ERK phosphorylation could be completely abolished by BX471, but not MVC, indicating that CCL5 activates the ERK signaling pathway through interaction with CCR1. Collectively, these results suggest that activated the CCL5/CCR1/ERK axis mediates the enhanced migratory ability toward glioma cells in De-neu-BMSCs.

Histone Modifications of CCL5 and Other Chemokines in De-neu-BMSCs

We have shown that De-neu-BMSCs are endowed with augmented CCL5/CCR1/ERK signaling, which contributes to their enhanced migratory ability. Next, we attempted to understand how this chemokine axis is upregulated in De-neu-BMSCs. Intriguingly, we have noticed that, while it has been reported that human and mouse MSCs routinely express low levels of selected chemokines and receptors (Honczarenko et al., 2006; Ringe et al., 2007), multiple chemokines are globally upregulated in De-neu-h/mBMSCs as well as CCL5 (Figures S2A and S2B). The upregulation of multiple chemokines in De-neu-h/mBMSCs cannot be explained by increased expression of TNF-α or activation of nuclear factor κB (NF-κB) per se, as we did not find significant differences in TNF-α secretion or NF-κB transcriptional activity between hBMSCs and De-neu-hBMSCs (Figures S2D and S2E). Since the epigenetic regulatory mechanism has been emerging as a key mechanism leading to the activation of gene transcription via modifications of chromatin architecture, we therefore evaluated gene-specific chromatin configurations using chromatin immunoprecipitation (ChIP) assays. In general, the binding levels of active H3 trimethyl lysine 4 (H3K4me3) and repressive histone H3 trimethyl lysine 27 (H3K27me3) on the promoters of chemokines tested are similar. Conversely, acetylated histone H4 (H4Ac), a mark of active gene transcription, occupied more on the promoter regions of chemokines than other histone markers indicating that these chemokines are probably more susceptible to histone acetylation-mediated regulation. Intriguingly, dedifferentiation treatment increased the *ccl5* promoter level of H3K4me3, but not H3K27me3. In addition, an elevated level of H4Ac was also seen on the *ccl5* promoter in De-neu-mBMSCs compared with unmanipulated mBMSCs (Figure 3A), indicating the activated status of related chemokines. In addition, the *cxcl2*, *cxc10*, *cxc11*, *il-6*, and *c3* promoters also showed increased H4Ac and/or H3K4me3 occupancy in De-neu-mBMSCs compared with naive mBMSCs (Figures 3B–3F), suggesting a shared pathway for maximizing chemokine expression. As a quality control, both cell populations showed inverse patterns of H3K4me3 and H3K27me3, H4Ac, and HDAC occupancies respectively on the *Gapdh* promoter, as expected from the high constitutive expression level of this gene (Figure 3G). It should be noted that there is no difference in H3K4me3 or H4Ac occupancy on the *tnf-α* promoter (Figure 3H), suggesting that this epigenetic regulatory mechanism is gene specific.

De-neu-BMSCs Are More Responsive to Tumor Growth Factors in Chemokine Induction and Migration

If De-neu-BMSCs are endowed with a more activated histone modification status at the promoter region of chemokines, the transcription of chemokines should be more susceptible to being activated. Thus, we evaluated the secretion of chemokines in mBMSCs or De-neu-mBMSCs in response to various growth factors and cytokines. As shown in Figure 4A, while the growth factors or cytokines mildly increased the expression levels of *ccl5* in unmanipulated mBMSCs, the upregulation of *ccl5* was more robust in De-neu-mBMSCs, indicating that De-neu-mBMSCs are more poised to produce ccl5 upon stimulation. The expression pattern of *cxcl10* was similar to that of *ccl5*, in response to platelet-derived growth factor-BB (PDGF-BB) and TNF-α (Figure S3A). Together, these results suggest that chemokine expression in De-neu-mBMSCs is more prone to being activated. In glioma, various growth factors such as PDGF-BB, stromal cell-derived factor 1 alpha, and epidermal growth factor (EGF) have been shown to attract MSCs by binding to their specific receptors expressed on MSCs. To determine whether BMSCs and De-neu-BMSCs exhibit differential chemotactic effects toward glioma growth factors, we added either EGF or PDGF-BB in the lower chamber of the transwell and determined the migratory ability of mBMSCs or De-neu-mBMSCs toward them. Our result showed that De-neu-mBMSCs were more attracted by EGF or PDGF-BB than unmanipulated mBMSCs (Figure 4B). To further confirm that the enhanced chemotaxis effect exhibited in De-neu-BMSCs is attributed to increased expression of *ccl5*, but not the interaction between tumor growth factors and their receptors, we knocked down *ccl5* in De-neu-mBMSCs and evaluated their chemotactic effects to PDGF-BB. Our result showed that knock down of *ccl5* completely reversed the enhanced chemotaxis effect toward PDGF-BB in De-neu-mBMSCs (Figure 4C).

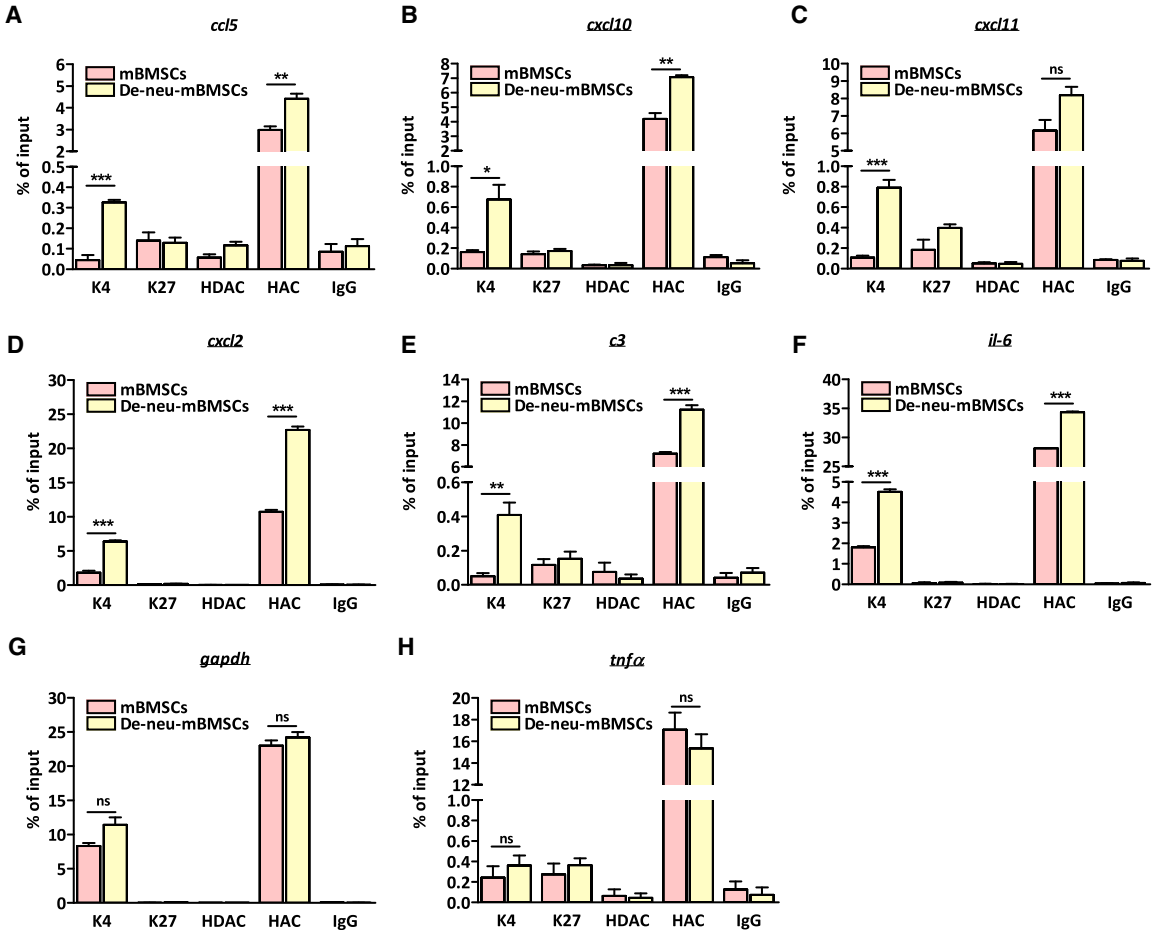

Figure 3. Chromatin Configurations of Chemokines in BMSCs Compared with De-neu-BMSCs

Note the increased occupancy of H3K4me3 and H4ac on the promoters of chemokines (A–H). The histone modifications of chemokine promoters were analyzed by ChIP-PCR assay. ChIP was done using anti-H3K4me3, anit-H3K27, HDAC, and anti-H4ac monoclonal antibodies, and PCR was performed with the primers listed in Table S1. Normal rabbit IgG was used as a negative control. Values are expressed as means ± SD of three independent experiments (*p < 0.05, **p < 0.01, ***p < 0.001).

In addition, neutralizing antibody of PDGF receptor did not have any effect on the enhanced chemotactic effect toward U87 cells in De-neu-mBMSCs (Figure S3B). Taken together, these results suggest that De-neu-BMSCs are more responsive to tumor growth factor-stimulated chemokine secretion and chemotaxis. Next, we asked whether the enhanced responsiveness shown in De-neu-mBMSCs is related to histone modification. We determined H4ac occupancy in *ccl5* and *cxcl10* promoter in response to EGF and PDGF-BB. Our results showed that both EGF and PDGF-BB significantly increased the occupancy of H4ac in the promoter regions of *ccl5* and *cxcl10*, which could be dramatically reversed by an HAT inhibitor, anacardic acid (Figures 4D and 4E). To determine whether epigenetically regulated chemokines functionally contribute to the migration of BMSCs, the migratory capacity toward U87 CM was determined in mBMSCs and De-neu-mBMSCs pre-treated with another HAT inhibitor, curcumin. The result showed that the enhanced migratory ability in De-neu-mBMSCs was completely reversed by curcumin (Figure 4F). Altogether, these results indicate that dedifferentiation-mediated reprogramming confers epigenetic plasticity to De-neu-BMSCs for chemokine activation, which contributes to the enhanced migratory behavior exhibited by these cells.

De-neu-BMSCs Exhibit Enhanced Migratory Potential In Vivo

Having established that De-neu-BMSCs are endowed with enhanced homing ability to glioma cells in vitro, we proceeded to compare the migratory and tumor-targeting capacities between BMSCs and De-neu-BMSCs in a glioma

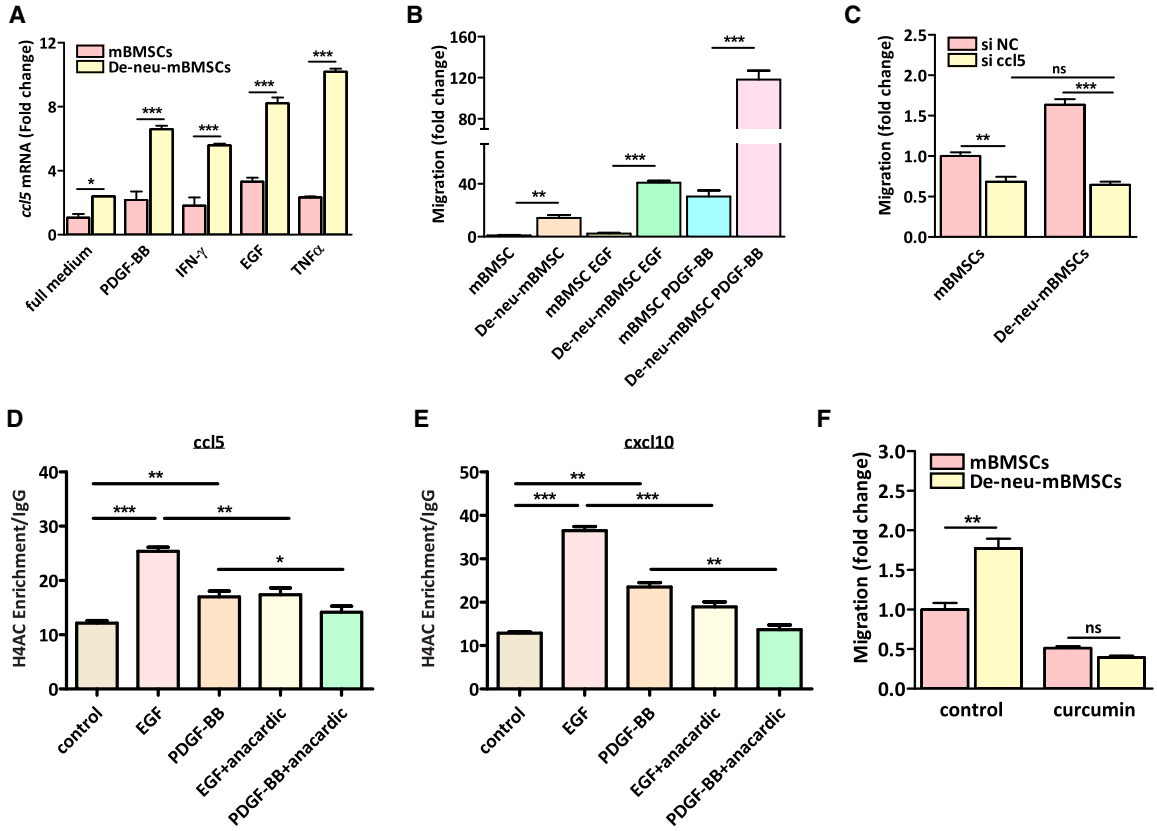

Figure 4. De-neu-BMSCs Are More Responsive to Tumor Growth Factors in Chemokine Expression and Migration

(A) *ccl5* mRNA expression in mBMSCs and De-neu-mBMSCs in response to 10% FBS, 10 ng/mL PDGF-BB, 10 ng/mL IFN-γ, 20 ng/mL EGF, or 80 pg/mL TNF-α was examined by real-time PCR. Quantification data are presented as means ± SD from three independent experiments (*p < 0.05, ***p < 0.001).

(B) The migratory ability of mBMSCs and De-neu-mBMSCs toward 10 ng/mL PDGF-BB or 20 ng/mL EGF was determined by transwell assay. Quantification data are presented as means ± SD from three independent experiments (**p < 0.01, ***p < 0.001).

(C) mBMSCs/De-neu-mBMSCs were treated with *ccl5* siRNA, and then examined for their migratory ability toward PDGF-BB (15 ng/mL). Quantification data are presented as means ± SD from three independent experiments (**p < 0.01, ***p < 0.001). ns, not significant.

(D) The histone modifications of *ccl5* promoter were analyzed by ChIP-PCR assay. The MSCs were treated with 10 ng/mL PDGF-BB or 20 ng/mL EGF with or without arachnoid acid for 24 hr. ChIP was done using anti-H4ac monoclonal antibodies, and PCR was performed with the primers listed in Table S1 (*p < 0.05, **p < 0.01, ***p < 0.001).

(E) The histone modifications of *cxcl10* promoter were analyzed by ChIP-PCR assay. The BMSCs were treated with 10 ng/mL PDGF-BB or 20 ng/mL EGF with or without arachnoid acid for 24 hr. ChIP was done using anti-H4ac monoclonal antibodies, and PCR was performed with the primers listed in Table S1 (**p < 0.01, ***p < 0.001).

(F) The migratory ability of mBMSCs and De-neu-mBMSCs toward U87 CM was tested by transwell assay after treatment with the HAT inhibitor curcumin (20 μM). Quantification data are presented as means ± SD from three independent experiments (**p < 0.01).

xenograft model. For the direct tracing of BMSCs or De-neu-BMSCs in animals, we took advantage of GFP-rat (rBMSCs-GFP), which was established in our lab. Our results showed that rBMSCs-GFP exhibited the same morphology change as normal human or mouse MSCs during the neural differentiation and dedifferentiation (Figure S4A). After dedifferentiation, De-neu-rBMSCs-GFP also showed enhanced migratory ability toward U87 CM as determined by transwell assay (Figure S4B). To determine the extent to which rBMSCs-GFP or De-neu-rBMSCs-GFP are capable of selectively integrating into human gliomas after delivery in vivo, intracranial xenografts of U87 were established in the frontal lobes of nude mice. Seven days after tumor inoculation, 1×10^5 rBMSCs-GFP or De-neu-rBMSCs-GFP were injected into the contralateral side of the brain to monitor long-distance tumor tropism in vivo (Figure 5A). Animals were killed 7 and 11 days after stem cell injection, the brains were removed, and frozen sections

were analyzed by direct visualization of GFP-positive cells under fluorescent microscopy. Our results showed that on the seventh day after stem cell injection in the contralateral side, while both rBMSCs-GFP and De-neu-rBMSCs-GFP migrated toward glioma loci which were located on the other side of the brain, De-neu-rBMSCs-GFP moved faster than rBMSCs-GFP, as a large portion of De-neu-rBMSCs-GFP already reached the contralateral hemisphere (Figure 5B, the yellow line indicate the boundary of right and left hemisphere). Strikingly, on the 11th day, half of the GFP-labeled cells were exclusively seen within the U87 tumor mass in De-neu-rBMSCs-GFP group (Figure 5C). In addition, some of the De-neu-rBMSCs-GFP already migrated to the border region of the glioma (Figure S4C). In contrast, rBMSCs-GFP remained at the corpus callosum region and did not show further migration toward the glioma (Figure 5C). These results indicate that De-neu-rBMSCs-GFP are more specifically attracted by glioma cells. The enhanced homing ability of De-neu-rBMSCs-GFP was further supported by experiments in which GFP-labeled rBMSCs/De-neu-rBMSCs were injected into the ipsilateral hemisphere to monitor short-distance migration. Seven days after U87 cells were injected into the mouse striatum (2 mm lateral and 1 mm anterior to bregma at a 3 mm depth from the skull base), rBMSCs-GFP or De-neu-rBMSCs-GFP were injected posterior to the tumor injection site in the ipsilateral hemisphere (2.8 mm lateral and 1 mm posterior to bregma at a 2.5 mm depth from the skull base, Figure S4D). As shown in Figures S4E and S4F, GFP^+ cells could be observed much far away from injected sites in the De-neu-rBMSCs-GFP group compared with those in the rBMSCs-GFP group. In addition, there are more De-neu-rBMSCs-GFP in the glioma mass (Figure S4G).

Next, we determined the expression of H4Ac to see whether the enhanced tumor capacity of De-neu-rBMSCs was associated with epigenetic-mediated regulation. As shown in Figure 5D, the expression level of H4Ac was dramatically increased in De-neu-rBMSCs compared with rBMSCs, indicating that upregulation of H4Ac might be related to the increased tumor-homing effect of De-neu-rBMSCs in vivo. To further affirm the effect of H4Ac-mediated regulation on BMSC migration, we stimulated BMSCs with a histone deacetylase inhibitor, valproic acid (VPA), and found that VPA (0.5–1 μM) significantly increased BMSC migration (Figure S5A). In addition, the CCR1 antagonist, BX471, significantly reversed VPA-induced migration, indicating that VPA-stimulated migration is mediated by the CCL5/CCR1 axis (Figure S5B). To further demonstrate that the CCL5/CCR1 signaling pathway, regulated by epigenetic modification, contributes to the enhanced homing capacity in vivo, we used a subcutaneous xenograft model and traced the BMSC homing effect using an IVIS 200 imaging system. Our results showed that VPA significantly enhanced the tumor-homing capacity of mBMSCs toward glioma, the effect of which was completely reversed by BX471 (Figure 6A). Taken together, these data demonstrate that the epigenetic regulation of CCL5/CCR1 axis contributes to the BMSC glioma homing effect in vivo.

De-neu-BMSCs Exhibit Enhanced Glioma-Targeting Effect In Vivo

With the demonstrated enhanced homing ability of De-neu-BMSCs both in vitro and in vivo, we reason that De-neu-BMSCs may function as a better gene delivery vehicle by eliciting enhanced tumor-targeting effects. The 5-fluorocytosine (5-FC)/*Escherichia coli* cytosine deaminase (CD) system is a suicide gene therapy system that is extensively used for malignant tumors (Fischer et al., 2005; Ichikawa et al., 2000; Mullen et al., 1992). Expression of the CD gene within the target sites produces an enzyme that converts the prodrug, 5-FC, to the toxic metabolite, 5-fluorouracil. Of interest, it was reported that MSCs expressing CD exhibited strong glioma-killing effects and significantly prolonged animal survival (Fei et al., 2012; Kosaka et al., 2012). As a first step to evaluate the therapeutic effect of de-differentiated human BMSCs in glioma targeting, we determined the anti-tumor effects of 5-FC/CD gene therapy with hBMSCs/De-neu-hBMSCs in this study. We first examined the cytotoxic effects of 5-FC/CD in vitro by co-culturing CD-hBMSCs with U87-expressing luciferase (U87-Luc). Our result showed that, while there was no cytotoxicity observed on the second day of co-culture, 5-FC/CD/hBMSCs caused significant cell death in U87 cells on the fourth day of co-culture in a dose-dependent manner (Figure S5C), indicating that our 5-FC/CD/hBMSCs system is valid for glioma killing. Next, we determined whether CD-expressing De-neu-hBMSCs along with 5-FC would show better anti-tumor effects compared with CD-hBMSCs. Considering that local injection of therapeutic stem cells after surgical resection would be more feasible, we decided to inject the therapeutic hBMSCs/De-neu-hBMSCs directly into the glioma xenografts. Five days after U87-LUC inoculation, CD-hBMSCs/CD-De-neu-hBMSCs were injected directly into the brain. Luciferin intensity was tested on the fourth and ninth day by IVIS 200 imaging after stem cell injection. Our in vivo luciferase tracing experiment indicated that, while CD-hBMSCs had mild inhibitory effects on glioma growth, CD-De-neu-hBMSCs significantly inhibited glioma growth in vivo (Figure 6B). In addition, we showed that CD-expressing De-neu-hBMSCs along with 5-FC treatment resulted in abundant apoptotic cell death in the tumor sites. More interestingly, the expression of Bax which is a pro-apoptotic gene, was dramatically increased in the tumor region upon suicide gene treatment with the De-neu-hBMSCs (Figure 6C). Taken together, these data suggest that reduction in tumor

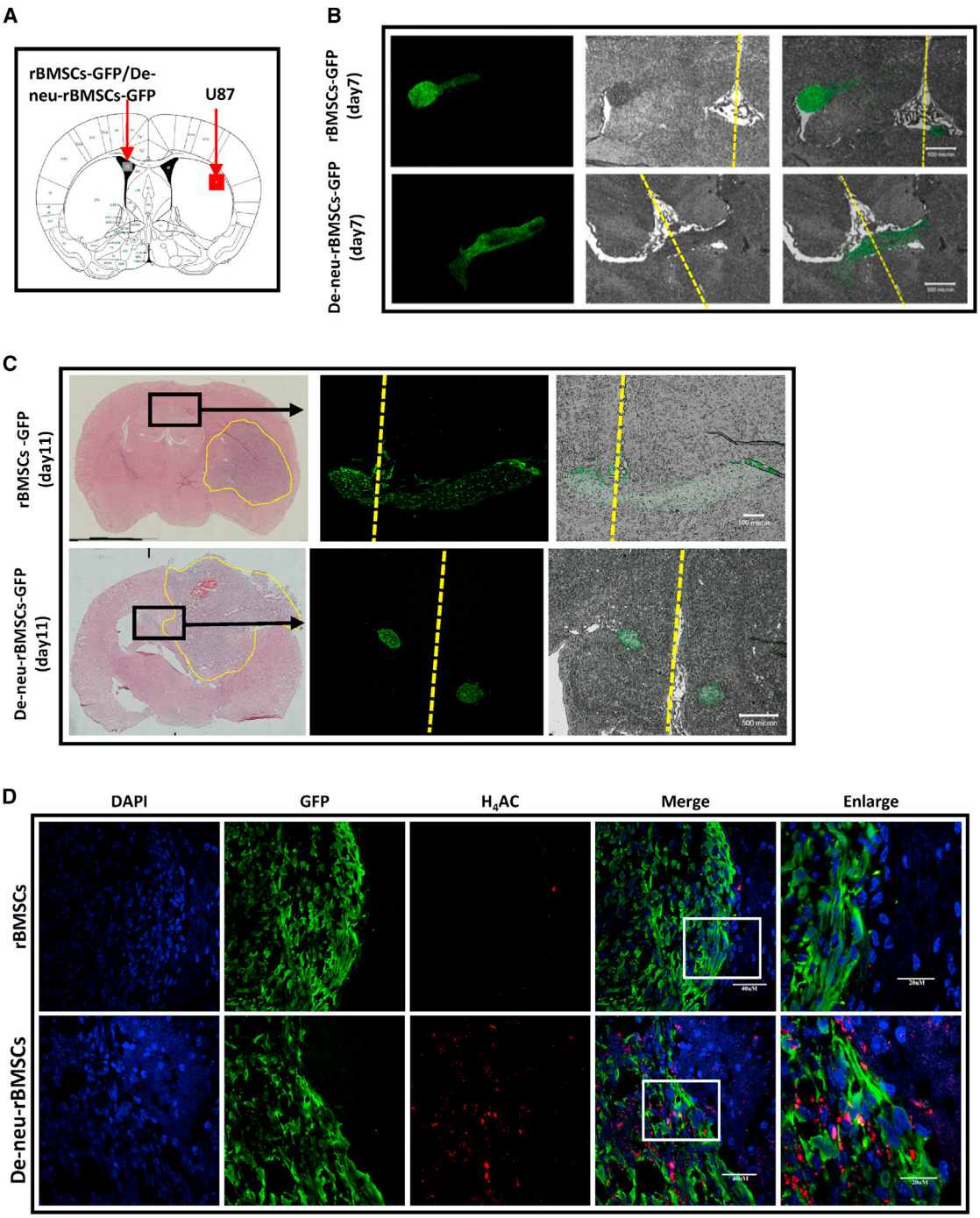

Figure 5. De-neu-BMSCs Exhibit Enhanced Tumor-Homing Capacity In Vivo

(A) Diagram illustration of a mouse brain coronal section shows the injection sites of U87 and rBMSCs-GFP/De-neu-rBMSCs-GFP. U87 cells were injected into the left hemisphere and rBMSCs-GFP/De-neu-rBMSCs-GFP were injected into the lateral ventricle of the right hemisphere.

(B) Seven days after stem cell injection, mouse brains were subjected to cryosections and rBMSCs-GFP/De-neu-rBMSCs-GFP that migrated toward tumor cells were checked under a fluorescence microscope (yellow line indicates the boundary of two hemispheres). Scale bars, 500 μm.

(C) Eleven days after stem cell injection, brain cryosections were subjected to H&E staining to illustrate tumor mass. Contralateral migration of rBMSCs-GFP/De-neu-rBMSCs-GFP toward tumor cells was determined under a fluorescence microscope; rBMSCs-GFP did not

(legend continued on next page)

mass in the CD-De-neu-hBMSC group was associated with apoptotic cell death.

DISCUSSION

While our previous study demonstrated that De-neu-BMSCs exhibited stronger anti-apoptosis ability and higher neuronal differentiation potential, our present work has revealed that De-neu-BMSCs are endowed with enhanced migratory and tumor-homing ability as well. This feature is critical for the therapeutic value of BMSC in cancer targeting, considering that BMSCs must migrate to tumor sites to exert their function. In our transwell assay, De-neu-BMSCs are more attracted by PDGF-BB and EGF (Figure 4B), which are highly secreted by various types of cancer cells. It should be noted that the origin of U87 has been questioned recently (Dolgin, 2016) and, while we used U87 as glioma model and focused on glioma in this study, it is very likely that the enhanced tumor tropic effect exhibited by De-neu-BMSCs is not limited to glioma. Indeed, we have found that besides glioma, De-neu-BMSCs exhibit enhanced migratory ability toward different types of cancer cells (Figure 1E). On the other hand, inflammation plays a critical role in every stage of tumor progression, and pro-inflammatory cytokines in the tumor microenvironment are crucial in modulating the tumor-homing effects of MSCs (Grivennikov et al., 2010). Of note, De-neu-BMSCs show an enhanced chemotaxis effect toward TGF-β_1 and interferon γ as well (Figures S3C and S3D), indicating that pro-inflammatory cytokines existing in the inflammatory milieu of the tumor microenvironment may contribute to the increased recruitment of De-neu-BMSCs in situ. Consistent with the in vitro data, we have demonstrated that De-neu-BMSCs present augmented glioma-tropic effects in the orthotopic xenograft mouse model (Figure 5). While unmanipulated rBMSCs-GFP show limited homing ability, De-neu-rBMSCs-GFP can specifically migrate to the other side of the brain and integrate into the tumor mass. Furthermore, De-neu-hBMSCs elicit stronger glioma-killing effects together with CD/5-FC compared with unmanipulated hBMSCs (Figure 6). These results clearly indicate that the dedifferentiation strategy augments the tumor-homing ability of BMSCs, which is pivotal for the application of BMSC-based adjuvant therapy for cancer.

Chemokines play a vital role in a biologic plethora of migration and are considered as guided cues for directional trafficking of stem cells (Wang and Knaut, 2014). Although CCL5 is a well-known pro-inflammatory chemokine that recruits white blood cells into inflammatory sites, and thereby has been believed to function in a paracrine manner (Marques et al., 2013), the present results have clearly revealed a pivotal role of the autocrine CCL5/CCR1/ERK axis in regulating cell migration in BMSCs, the alteration of which contributes to the differences observed between De-neu-BMSCs and BMSCs (Figure 2). More importantly, we have provided evidence that histone modification is involved in the regulation of chemokine activation in BMSCs. The increase of core active histone markers indicates that the chromatin structure on chemokine promoters becomes loose and open, making De-neu-BMSCs more predisposed for activation. It should be noted that H4ac, a marker of active gene transcription, occupies more on the promoter regions of chemokines than other histone markers, indicating that these chemokines are more susceptible to acetylation-mediated regulation. This result is consistent with the other reports showing that acetylation modification patterns are more responsive to culture condition in MSCs (Fani et al., 2016; Zhu et al., 2015). Moreover, in our previous study, we observed that the expression of multiple histone acetyltransferases was markedly increased in dedifferentiated-reprogrammed BMSCs (Rui et al., 2015). Consistently, in this study, we demonstrated that the expression of H4Ac was also significantly increased in the migrating De-neu-BMSCs toward glioma in vivo (Figure 5D). Based on these findings, we speculate that increased histone acetylation of key chemokine might contribute to the gene activation and enhanced migratory capability in De-neu-BMSCs. Indeed, the occupancy of H4ac on chemokine promoters is significantly increased upon growth factor stimuli (Figures 4D and 4E), and the enhanced migratory ability exhibited in De-neu-BMSCs is completely reversed by an HAT inhibitor, curcumin (Figure 4F). Furthermore, the VPA-induced tumor-homing effect could be completely alleviated by the CCR1 inhibitor (Figure 6A). Taken together, our results provide the documentation that the chemokine axis in MSCs is subject to histone modification-mediated epigenetic regulation, and that such a regulation can significantly influence the migratory capacity for homing of MSC. This demonstration raises questions regarding how the active histone markers are targeted to select chemokine genes and whether related pathways control MSC access to the

migrate into the tumor site, whereas a large amount of De-neu-rBMSCs-GFP migrated into the tumor mass. Scale bars, 100 μm (upper panel) and 500 μm (lower panel).

(D) Immunofluorescent staining of H4Ac shows that the expression of H4Ac (red) is significantly increased in De-neu-rBMSCs-GFP cells. The yellow line indicates the tumor margin next to the De-neu-rBMSCs-GFP. The white square is enlarged on the right. Scale bars, 40 μm and 20 μm.

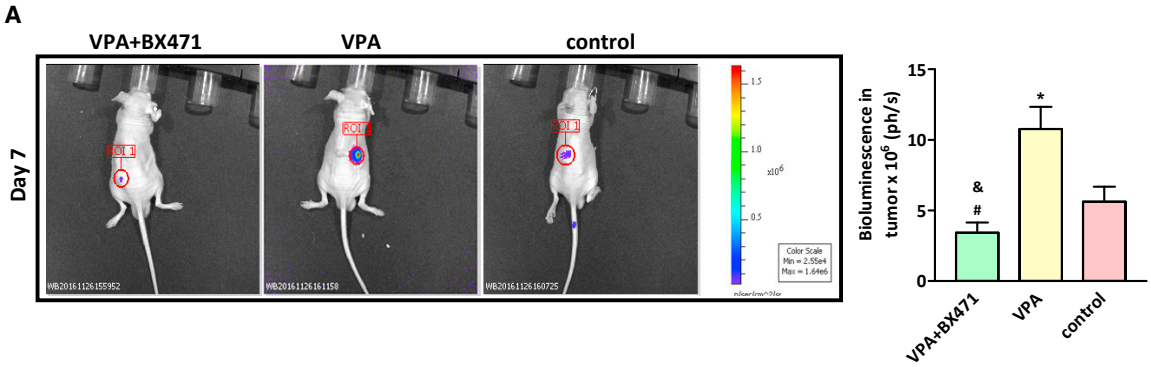

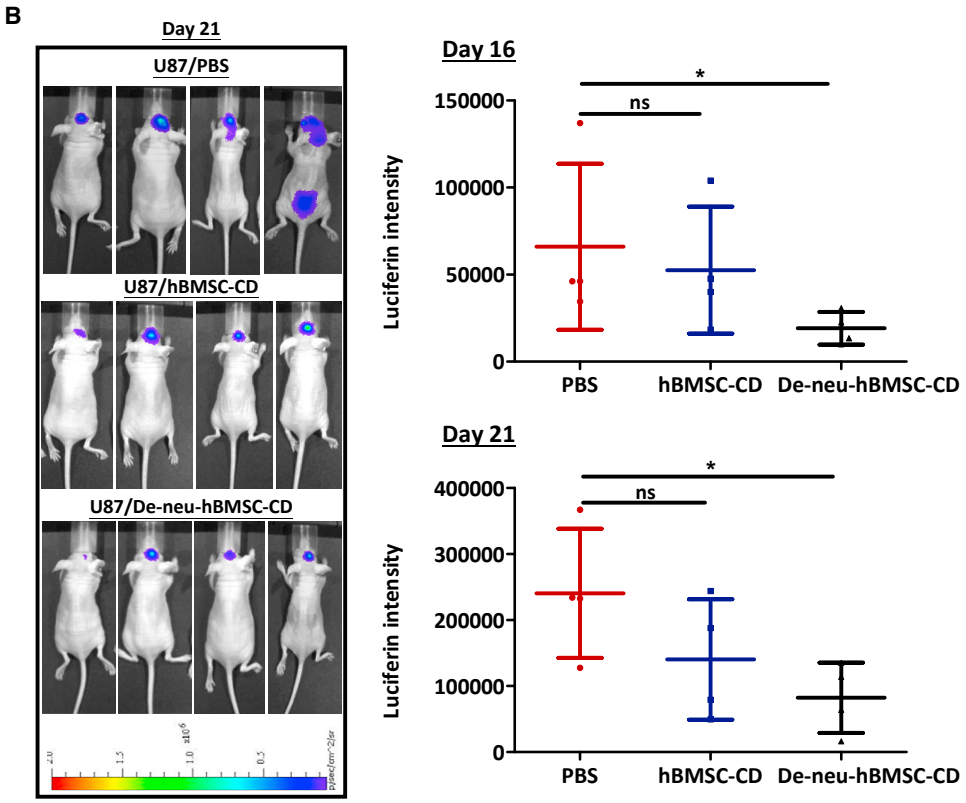

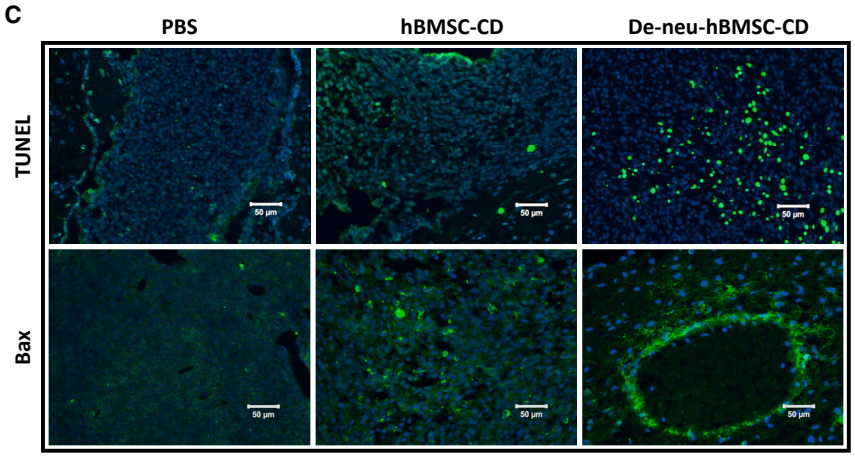

(legend on next page)

stroma of infected, autoimmunity-afflicted, or cancer-bearing tissues. Conversely, aberrant chemokine silencing by suppressive histone modification may influence the mobility and responsiveness of the MSC to injury and subsequent repair process.

In closing, the present study has revealed that the in vitro culture strategy through neuronal differentiation and dedifferentiation has reprogrammed BMSCs with enhanced migratory capacity and homing ability toward cancer, the effect of which is mediated by the CCL5/CCR1/ERK pathway. The epigenetic mechanism involving histone modification endows reprogrammed BMSCs with epigenetic plasticity by opening up the chromatin structure at the genes encoding Th1/Tc1-attracting chemokines. The findings of this study have the potential to greatly enlarge the number of tumor-targeting MSCs, and thereby enhance the tumor-killing efficacy of anti-cancer agents, which provides grounds for the ultimate application of dedifferentiation-reprogrammed cell-based or histone modification-based tumor-targeting gene therapy for various cancers in the future. However, the finding that chemokine expression in MSCs could be regulated by histone modification provides an insight into the chemokine regulation in MSCs, which may have more profound effects on MSC function, considering that the chemokine axis is critical for the paracrine effect of MSCs. Focused efforts on the detailed mechanisms linking the epigenetic regulatory mechanisms to MSC chemokine secretion in physiological/pathological conditions could have a broad impact on the application of MSCs in regenerative medicine and cancer targeting.

EXPERIMENTAL PROCEDURES

Animal Models

Glioma Xenografts and Stem Cell Transplantation

Mice were obtained from the Laboratory Animal Service Center (LASEC) of the Chinese University of Hong Kong (CUHK). All animal work was performed with the approval and followed the guidelines of the Animal Experimentation Ethics Committee of The Chinese University of Hong Kong.

Eight-week-old nude mice were anesthetized by intraperitoneal injection of a ketamine (75 mg/kg) and xylazine (10 mg/kg) mixture. U87 cells (5×10^4 in 3 μL of PBS) were stereotactically injected via a 30-gauge Hamilton syringe (Hamilton) into the right striatum (2.0 mm lateral, 1.0 mm anterior to bregma, 3.0 mm depth from the skull surface) within 3 min, 7 days after U87 cell injection, rBMSCs-GFP/De-neu-rBMSCs-GFP (5×10^5 cells in 5 μL of PBS) were injected into the ipsilateral hemisphere to the tumor (2.8 mm lateral, 1.0 mm posterior to bregma, 3.3 mm depth from the skull surface), or the contralateral hemisphere to the tumor (−2.0 mm lateral, 1.0 mm anterior to bregma, 3.0 mm depth from the skull surface) as indicated. Seven or 11 days after rBMSCs-GFP/De-neu-rBMSCs-GFP injection, mice were killed and rBMSCs-GFP/De-neu-BMSCs-GFP migration was detected by GFP^+ cells from brain series cryosection under fluorescence microscope. For cryosection preparation, mouse brains were fixed with 4% paraformaldehyde perfusion, dehydrated by sequential immersion into 10%, 20%, and 30% sucrose solution. Then tissues were embedded into an OCT gel, and stored at −80°C. OCT blocks were cut into 5 μm sections in the cryostat (Thermo Scientific) at −20°C.

BMSC-CD/5-FC Glioma Targeting

A total of 5×10^4 U87-Luc cells were injected into the right striatum (2.0 mm lateral, 1.0 mm anterior to bregma, 3.0 mm depth from the skull surface) of nude mice. Seven days later, 5×10^5 hBMSCs/De-neu-hBMSCs-CD were injected into the same coordinate as U87-Luc. Animals were intraperitoneally treated with 50 mg/kg/day 5FC diluted in PBS, 2 days after of stem cell injection. The injections were repeated twice for 5 consecutive days with a 2-day break. To examine the growth of glioma using the IVIS 200 system (Xenogen, Caliper Life Sciences), D-luciferin (150 mg/kg) was administered intraperitoneally 5 min before the imaging examination. The animals were anesthetized using 3% isoflurane and placed inside the camera box. The light emitted from the bioluminescent tumor cells was digitized and electronically displayed as a pseudocolor overlay onto the gray-scale animal image. Regions of interest were drawn around the tumor and quantified as photons per second using the software provided.

Figure 6. Anti-Tumor Effect of hBMSC-CD/De-neu-hBMSC-CD in a Xenograft Animal Model

(A) Tumor implants were established by subcutaneous injection of 8×10^5 U87 cells at the dorsal site of nude mice. Luc-BMSCs (5×10^5) in 50 μL of PBS was injected intravenously at day 5 in the subcutaneous tumor model. The distribution of Luc-BMSCs were examined by the IVIS 200 system at day 7 after injection of Luc-BMSCs ($^*p < 0.05$ compared with control, $^{\#}p < 0.05$ compared with VPA, $^{\&}$ indicates not significant compared with control; n = 3).

(B) Anti-tumor effect of locally administered hBMSC-CD/De-neu-hBMSC-CD in the presence of 5-FC in U87 tumor-transplanted mice was determined. A total of 5×10^4 U87-Luc cells were injected into the right striatum (2.0 mm lateral, 1.0 mm anterior to bregma, 3.0 mm depth from the skull surface) of nude mice. Seven days later, 5×10^5 hBMSCs/De-neu-hBMSCs-CD were injected into the same coordinates as U87-Luc. Left: in vivo real-time tracking of bioluminescence imaging at day 21 after tumor implantation using an IVIS Xenogen camera. Right: at days 16 and 21 after tumor implantation, tumor volume was significantly smaller in the De-neu-hBMSC-CD + 5-FC group ($^*p < 0.05$, n = 4).

(C) TUNEL staining and immunofluorescent staining of Bax show increased apoptotic response in De-neu-hBMSC-CD-treated tumor lesions. DAPI stains for nuclear DNA. Scale bars, 50 μm.

Subcutaneous Mouse Model

Tumor implants were established by subcutaneous injection of 8×10^5 U87 cells at the dorsal site of nude mice. Luc-BMSCs (5×10^5) in 50 μL of PBS was injected intravenously at day 5 in the subcutaneous tumor model. The distribution of Luc-BMSCs were examined by the IVIS 200 system at days 7 or 14 after injection of Luc-BMSCs.

SUPPLEMENTAL INFORMATION

Supplemental Information includes Supplemental Experimental Procedures, five figures, and one table and can be found with this article online at http://dx.doi.org/10.1016/j.stemcr.2017.01.016.

ACKNOWLEDGMENT

This work is supported by the National Natural Science Foundation of China (NSFC no. 81272548), the National 973 project (2013CB967401), and the Hong Kong Food and Health Bureau (01120056, 01120306, 03140496). The work is also supported in part by the SMART program seed funding to X.J., G.L., and H.C.C., the Lui Che Woo Institute of Innovation Medicine, and The Chinese University of Hong Kong.

Received: August 10, 2016
Revised: January 15, 2017
Accepted: January 16, 2017
Published: February 16, 2017

REFERENCES

Aldinucci, D., and Colombatti, A. (2014). The inflammatory chemokine CCL5 and cancer progression. Mediators Inflamm. *2014*, 292376.

Alexeev, V., Donahue, A., Uitto, J., and Igoucheva, O. (2013). Analysis of chemotactic molecules in bone marrow-derived mesenchymal stem cells and the skin: Ccl27-Ccr10 axis as a basis for targeting to cutaneous tissues. Cytotherapy *15*, 171–184.e1.

Caplan, A.I. (2007). Adult mesenchymal stem cells for tissue engineering versus regenerative medicine. J. Cell Physiol. *213*, 341–347.

Dolgin, E. (2016). Venerable brain-cancer cell line faces identity crisis. Nature *537*, 149–150.

Donlon, T.A., Krensky, A.M., Wallace, M.R., Collins, F.S., Lovett, M., and Clayberger, C. (1990). Localization of a human T-cell-specific gene, RANTES (D17S136E), to chromosome 17q11.2-q12. Genomics *6*, 548–553.

Egea, V., von Baumgarten, L., Schichor, C., Berninger, B., Popp, T., Neth, P., Goldbrunner, R., Kienast, Y., Winkler, F., Jochum, M., et al. (2011). TNF-alpha respecifies human mesenchymal stem cells to a neural fate and promotes migration toward experimental glioma. Cell Death Differ. *18*, 853–863.

Eggenhofer, E., Luk, F., Dahlke, M.H., and Hoogduijn, M.J. (2014). The life and fate of mesenchymal stem cells. Front. Immunol. *5*, 148.

Eseonu, O.I., and De Bari, C. (2015). Homing of mesenchymal stem cells: mechanistic or stochastic? Implications for targeted delivery in arthritis. Rheumatology *54*, 210–218.

Fani, N., Ziadlou, R., Shahhoseini, M., and Baghaban Eslaminejad, M. (2016). Comparative epigenetic influence of autologous versus fetal bovine serum on mesenchymal stem cells through in vitro osteogenic and adipogenic differentiation. Exp. Cell Res. *344*, 176–182.

Fei, S., Qi, X., Kedong, S., Guangchun, J., Jian, L., and Wei, Q. (2012). The antitumor effect of mesenchymal stem cells transduced with a lentiviral vector expressing cytosine deaminase in a rat glioma model. J. Cancer Res. Clin. Oncol. *138*, 347–357.

Fischer, U., Steffens, S., Frank, S., Rainov, N.G., Schulze-Osthoff, K., and Kramm, C.M. (2005). Mechanisms of thymidine kinase/ganciclovir and cytosine deaminase/5-fluorocytosine suicide gene therapy-induced cell death in glioma cells. Oncogene *24*, 1231–1243.

Gibon, E., Yao, Z., Rao, A.J., Zwingenberger, S., Batke, B., Valladares, R., Smith, R.L., Biswal, S., Gambhir, S.S., and Goodman, S.B. (2012). Effect of a CCR1 receptor antagonist on systemic trafficking of MSCs and polyethylene particle-associated bone loss. Biomaterials *33*, 3632–3638.

Grivennikov, S.I., Greten, F.R., and Karin, M. (2010). Immunity, inflammation, and cancer. Cell *140*, 883–899.

Honczarenko, M., Le, Y., Swierkowski, M., Ghiran, I., Glodek, A.M., and Silberstein, L.E. (2006). Human bone marrow stromal cells express a distinct set of biologically functional chemokine receptors. Stem Cells *24*, 1030–1041.

Hong, X., Miller, C., Savant-Bhonsale, S., and Kalkanis, S.N. (2009). Antitumor treatment using interleukin- 12-secreting marrow stromal cells in an invasive glioma model. Neurosurgery *64*, 1139–1146, [discussion: 1146–7].

Ichikawa, T., Tamiya, T., Adachi, Y., Ono, Y., Matsumoto, K., Furuta, T., Yoshida, Y., Hamada, H., and Ohmoto, T. (2000). In vivo efficacy and toxicity of 5-fluorocytosine/cytosine deaminase gene therapy for malignant gliomas mediated by adenovirus. Cancer Gene Ther. *7*, 74–82.

Kauts, M.L., Pihelgas, S., Orro, K., Neuman, T., and Piirsoo, A. (2013). CCL5/CCR1 axis regulates multipotency of human adipose tissue derived stromal cells. Stem Cell Res. *10*, 166–178.

Kim, S.M., Lim, J.Y., Park, S.I., Jeong, C.H., Oh, J.H., Jeong, M., Oh, W., Park, S.H., Sung, Y.C., and Jeun, S.S. (2008). Gene therapy using TRAIL-secreting human umbilical cord blood-derived mesenchymal stem cells against intracranial glioma. Cancer Res. *68*, 9614–9623.

Kim, E.J., Kim, N., and Cho, S.G. (2013). The potential use of mesenchymal stem cells in hematopoietic stem cell transplantation. Exp. Mol. Med. *45*, e2.

Kosaka, H., Ichikawa, T., Kurozumi, K., Kambara, H., Inoue, S., Maruo, T., Nakamura, K., Hamada, H., and Date, I. (2012). Therapeutic effect of suicide gene-transferred mesenchymal stem cells in a rat model of glioma. Cancer Gene Ther. *19*, 572–578.

Lazarus, H.M., Koc, O.N., Devine, S.M., Curtin, P., Maziarz, R.T., Holland, H.K., Shpall, E.J., McCarthy, P., Atkinson, K., Cooper, B.W., et al. (2005). Cotransplantation of HLA-identical sibling culture-expanded mesenchymal stem cells and hematopoietic stem cells in hematologic malignancy patients. Biol. Blood Marrow Transpl. *11*, 389–398.

Lee, P.H., Kim, J.W., Bang, O.Y., Ahn, Y.H., Joo, I.S., and Huh, K. (2008). Autologous mesenchymal stem cell therapy delays the progression of neurological deficits in patients with multiple system atrophy. Clin. Pharmacol. Ther. *83*, 723–730.

Li, W., Ren, G., Huang, Y., Su, J., Han, Y., Li, J., Chen, X., Cao, K., Chen, Q., Shou, P., et al. (2012). Mesenchymal stem cells: a double-edged sword in regulating immune responses. Cell Death Differ. *19*, 1505–1513.

Lin, S.J., Chang, K.P., Hsu, C.W., Chi, L.M., Chien, K.Y., Liang, Y., Tsai, M.H., Lin, Y.T., and Yu, J.S. (2013). Low-molecular-mass secretome profiling identifies C-C motif chemokine 5 as a potential plasma biomarker and therapeutic target for nasopharyngeal carcinoma. J. Proteomics *94*, 186–201.

Liu, Y., Jiang, X., Yu, M.K., Dong, J., Zhang, X., Tsang, L.L., Chung, Y.W., Li, T., and Chan, H.C. (2010). Switching from bone marrow-derived neurons to epithelial cells through dedifferentiation and translineage redifferentiation. Cell Biol. Int. *34*, 1075–1083.

Liu, Y., Jiang, X., Zhang, X., Chen, R., Sun, T., Fok, K.L., Dong, J., Tsang, L.L., Yi, S., Ruan, Y., et al. (2011). Dedifferentiation-reprogrammed mesenchymal stem cells with improved therapeutic potential. Stem Cells *29*, 2077–2089.

Lu, L., Zhang, X., Zhang, M., Zhang, H., Liao, L., Yang, T., Zhang, J., Xian, L., Chen, D., and Wang, M. (2015). RANTES and SDF-1 are keys in cell-based therapy of TMJ osteoarthritis. J. Dental Res. *94*, 1601–1609.

Marques, R.E., Guabiraba, R., Russo, R.C., and Teixeira, M.M. (2013). Targeting CCL5 in inflammation. Expert Opin. Ther. Targets *17*, 1439–1460.

Marquez-Curtis, L.A., Qiu, Y., Xu, A., and Janowska-Wieczorek, A. (2014). Migration, proliferation, and differentiation of cord blood mesenchymal stromal cells treated with histone deacetylase inhibitor valproic acid. Stem Cell Int. *2014*, 610495.

Mullen, C.A., Kilstrup, M., and Blaese, R.M. (1992). Transfer of the bacterial gene for cytosine deaminase to mammalian cells confers lethal sensitivity to 5-fluorocytosine: a negative selection system. Proc. Natl. Acad. Sci. USA *89*, 33–37.

Nakamizo, A., Marini, F., Amano, T., Khan, A., Studeny, M., Gumin, J., Chen, J., Hentschel, S., Vecil, G., Dembinski, J., et al. (2005). Human bone marrow-derived mesenchymal stem cells in the treatment of gliomas. Cancer Res. *65*, 3307–3318.

Nakamura, K., Ito, Y., Kawano, Y., Kurozumi, K., Kobune, M., Tsuda, H., Bizen, A., Honmou, O., Niitsu, Y., and Hamada, H. (2004). Antitumor effect of genetically engineered mesenchymal stem cells in a rat glioma model. Gene Ther. *11*, 1155–1164.

Poloni, A., Maurizi, G., Leoni, P., Serrani, F., Mancini, S., Frontini, A., Zingaretti, M.C., Siquini, W., Sarzani, R., and Cinti, S. (2012). Human dedifferentiated adipocytes show similar properties to bone marrow-derived mesenchymal stem cells. Stem Cells *30*, 965–974.

Ringe, J., Strassburg, S., Neumann, K., Endres, M., Notter, M., Burmester, G.R., Kaps, C., and Sittinger, M. (2007). Towards in situ tissue repair: human mesenchymal stem cells express chemokine receptors CXCR1, CXCR2 and CCR2, and migrate upon stimulation with CXCL8 but not CCL2. J. Cell Biochem. *101*, 135–146.

Ripa, R.S., Haack-Sorensen, M., Wang, Y., Jorgensen, E., Mortensen, S., Bindslev, L., Friis, T., and Kastrup, J. (2007). Bone marrow derived mesenchymal cell mobilization by granulocyte-colony stimulating factor after acute myocardial infarction: results from the stem cells in myocardial infarction (STEMMI) trial. Circulation *116*, I24–I30.

Rui, Y., Xu, L., Chen, R., Zhang, T., Lin, S., Hou, Y., Liu, Y., Meng, F., Liu, Z., Ni, M., et al. (2015). Epigenetic memory gained by priming with osteogenic induction medium improves osteogenesis and other properties of mesenchymal stem cells. Scientific Rep. *5*, 11056.

Ryu, C.H., Yoon, W.S., Park, K.Y., Kim, S.M., Lim, J.Y., Woo, J.S., Jeong, C.H., Hou, Y., and Jeun, S.S. (2012). Valproic acid downregulates the expression of MGMT and sensitizes temozolomide-resistant glioma cells. J. Biomed. Biotechnol. *2012*, 987495.

Tian, Y., New, D.C., Yung, L.Y., Allen, R.A., Slocombe, P.M., Twomey, B.M., Lee, M.M., and Wong, Y.H. (2004). Differential chemokine activation of CC chemokine receptor 1-regulated pathways: ligand selective activation of Galpha 14-coupled pathways. Eur. J. Immunol. *34*, 785–795.

Tian, Y., Lee, M.M., Yung, L.Y., Allen, R.A., Slocombe, P.M., Twomey, B.M., and Wong, Y.H. (2008). Differential involvement of Galpha16 in CC chemokine-induced stimulation of phospholipase Cbeta, ERK, and chemotaxis. Cell Signal. *20*, 1179–1189.

Uccelli, A., Moretta, L., and Pistoia, V. (2008). Mesenchymal stem cells in health and disease. Nat. Rev. Immunol. *8*, 726–736.

Vanden Berg-Foels, W.S. (2014). In situ tissue regeneration: chemoattractants for endogenous stem cell recruitment. Tissue Eng. Part B Rev. *20*, 28–39.

Wang, J., and Knaut, H. (2014). Chemokine signaling in development and disease. Development *141*, 4199–4205.

Wise, A.F., Williams, T.M., Kiewiet, M.B., Payne, N.L., Siatskas, C., Samuel, C.S., and Ricardo, S.D. (2014). Human mesenchymal stem cells alter macrophage phenotype and promote regeneration via homing to the kidney following ischemia-reperfusion injury. Am. J. Physiol. Ren. Physiol. *306*, F1222–F1235.

Zhu, Y., Song, X., Han, F., Li, Y., Wei, J., and Liu, X. (2015). Alteration of histone acetylation pattern during long-term serum-free culture conditions of human fetal placental mesenchymal stem cells. PLoS One *10*, e0117068.